

Supporting Information

Scalable, low-cost synthesis of high volumetric capacity $\text{LiMn}_{0.5}\text{Fe}_{0.5}\text{PO}_4$ cathode for lithium-ion batteries

Seth Reed^a, Kevin Scanlan^a, and Arumugam Manthiram^{a,*}

^a Materials Science and Engineering Program & Texas Materials Institute, The University of
Texas at Austin, Austin, TX, 78712-1591 USA

*E-mail: rmanth@mail.utexas.edu

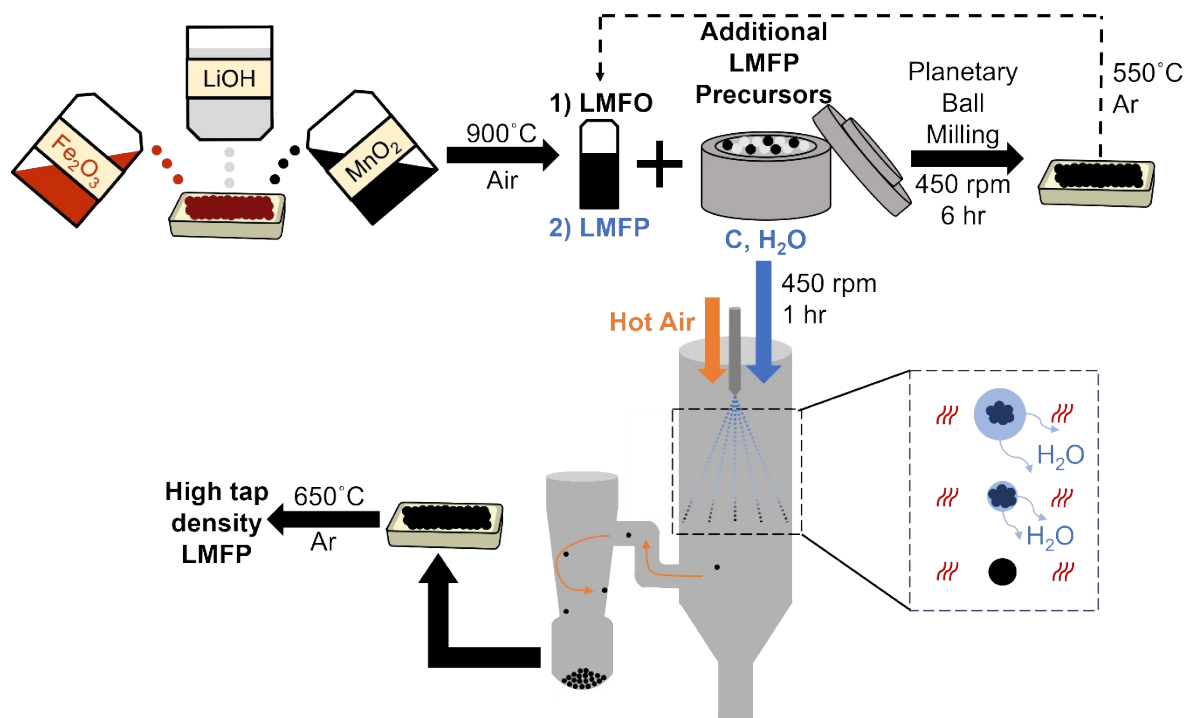


Fig. S-1. Two-step carbon coating synthesis process for S-LMFP. LMFO is synthesized and mixed with the additional precursors for LMFP and calcined to form an intermediate product. The intermediate product is mixed with more carbon and fed into the spray dryer as an aqueous solution, which upon calcination forms dense LMFP.



Fig. S-2. Mixed solution of $\text{Fe}_{0.5}\text{Mn}_{0.5}\text{O}$, $\text{NH}_4\text{H}_2\text{PO}_4$, and H_2O . The high viscosity indicates Mn^{2+} dissolution has caused byproducts to form that inherently affect the solution rheology.

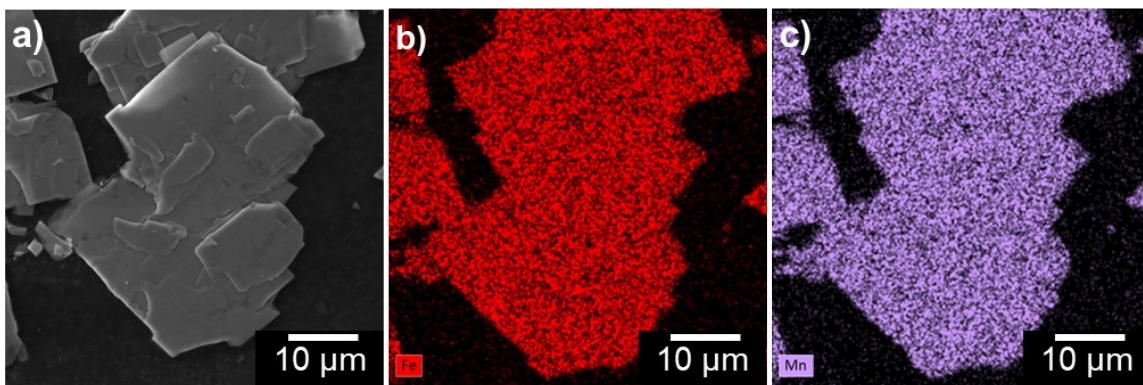


Fig. S-3. (a) SEM image of $\text{NH}_4\text{Mn}_{0.5}\text{Fe}_{0.5}\text{PO}_4$ with EDS mapping of (b) Fe and (c) Mn.

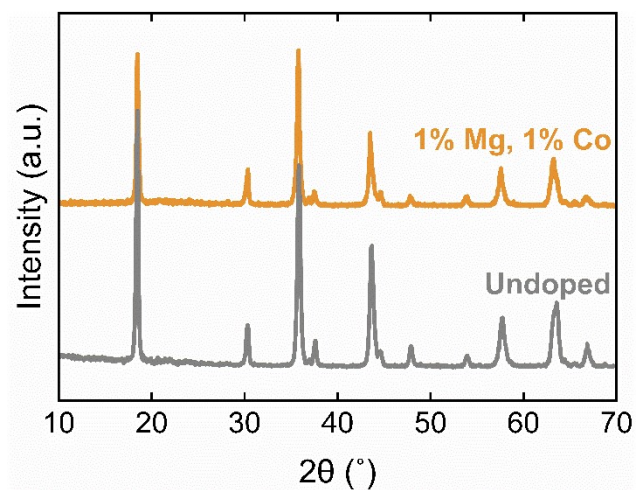


Fig. S-4. XRD patterns of pristine LMFO and LMFO doped with 1 mol% Mg and 1 mol% Co.

Table S-1. Lattice parameters and crystallite size values obtained from Rietveld refinement of

Sample	<i>a</i> (Å)	<i>b</i> (Å)	<i>c</i> (Å)	Crystal Size (nm)	R_{wp}
S-LMFP	4.72	10.40	6.05	152	10.2%
P-LMFP	4.72	10.38	6.05	151	10.0%

the XRD patterns of S-LMFP and P-LMFP cathodes

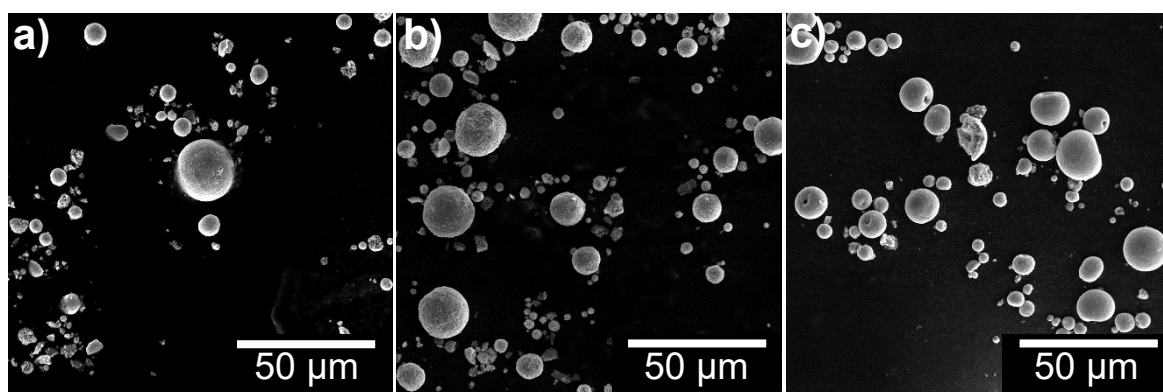


Fig. S-5. Low magnification SEM images of (a) S-LMFP, (b) P-LMFP, and (c) O-LMFP.

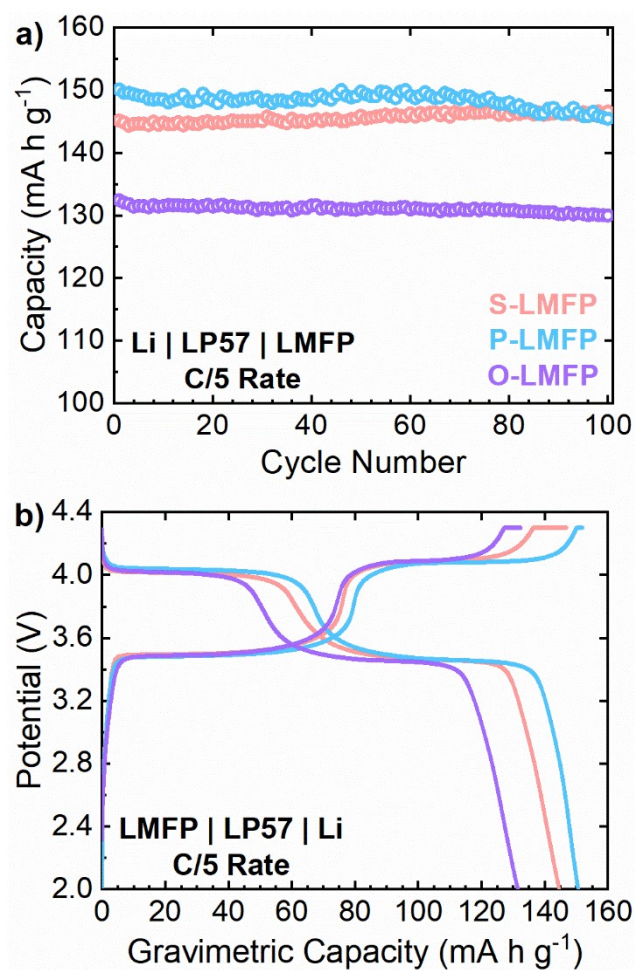


Fig. S-6. Electrochemical performances of all three LMFP samples on a gravimetric basis. (a) Half-cell cycling performances of all three LMFP samples and (b) voltage profiles recorded at C/5 charge and discharge rates. Aerial capacities of all the samples with 1.4 to 1.6 mA h cm⁻². The press densities of S-LMFP, P-LMFP, and O-LMFP are, respectively, 2.31, 1.93, and 2.40 g cm⁻³.